Benthic jellyfish dominate water mixing in mangrove ecosystems

David M. Durieux[a,1,2], **Kevin T. Du Clos**[a,1], **and Brad J. Gemmell**[a,1]

[a]University of South Florida, Department of Integrative Biology, 12037 USF Beard Drive, Tampa, FL, 33620

This manuscript was compiled on September 24, 2019

Water mixing affects aquatic ecosystem processes by regulating the interactions between water masses such as delivering nutrient-rich water to depleted areas. Physical processes, such as winds or tides, are primarily responsible for mixing effects in shallow coastal systems, but the sheltered flats adjacent to mangrove habitats experience very low turbulence and vertical mixing. The significance of animal biogenic mixing in open ocean habitats is unclear, but in this study we explore the role of the upside-down jellyfish *Cassiopea* sp., with respect to biogenic contribution to water column mixing in shallow, sheltered habitats. The mixing contribution was determined by means of high definition Particle Image Velocimetry (PIV) in both the laboratory and in the natural environment. *Cassiopea* sp. was found to continuously pump water from the benthos upward in a vertical jet with flow velocities in the range of 1 to 2 cm s^{-1}. The volumetric flow rate was found to be 212 l h^{-1} for average sized animals (8.6 cm bell diameter), leading to a water column turnover rate of about 15 minutes for a median population density (29 animals m^{-2}). In addition, *Cassiopea* sp. were responsible for release of porewater into the water column at an average rate of 2.64 ml h^{-1}. This release of benthic porewater, which is often nutrient-rich, in conjunction with the increase in water column mixing, suggest a role for *Cassiopea* sp. as an ecosystem engineer in mangrove habitats.

Cassiopea | Upside-down Jellyfish | Water Mixing | Particle Image Velocimetry | Nutrient Flux

Mangroves provide many ecosystem services, including control of flooding, sedimentation, and nutrient input in surrounding areas (1). In addition, mangroves act as critical nursery habitat for larvae of a wide range of commercially or ecologically important species of fish and crustaceans (2, 3) and as habitat for adults of many others (3). Biogenic mixing may be of particular importance in mangrove ecosystems, as these habitats experience comparatively little physical mixing due wind or tidal flow(4). Since water mixing regulates ecosystem processes such as productivity (5) and benthic-pelagic coupling (6) by altering nutrient availability, prey encounter rate, and gas exchange, it is important to understand the major sources of mixing in aquatic environments. Mixing forces can be environmental, such as wind or tides, or they can be biotic in origin. The growing field of biogenic mixing in the marine environment has explored the potential contributions of several taxa, including pelagic jellyfish, fish, and krill in the water column (7, 8), and bivalves in the benthos (9). While the primary source of turbulent mixing in shallow coastal ecosystems is wind-driven wave action (10), mangrove ecosystems provide shelter from wind and waves, as well as dampen mixing from tidal currents, which tend to run primarily in deeper channels within mangrove ecosystems. Therefore, physical mixing is naturally low in *Cassiopea* sp. habitat, implying that animal-mediated mixing could have substantial impacts on the local environment.

The upside-down jellyfish, *Cassiopea* sp., has a nearly circumtropical distribution (11). They are found in shallow, low energy coastal environments, often dominated by the red mangrove, *Rhizophora mangle* (12) and have been observed at high densities up to 31 animals m^{-2} or 20% benthic coverage (13). Not only is their natural range extensive, but it has further spread as an invasive species due to anthropogenic introduction (14–16) and natural range expansion, possibly due to rising ocean temperatures (15). In addition, it appears that *Cassiopea* sp. size and abundance have increased near anthropogenically disturbed habitats, where nutrients tend to be elevated (17).

Unlike other jellyfish, *Cassiopea* sp. exhibit a benthic lifestyle, laying with their bell on the substrate and oral arms facing up into the water column. They pulse their bells nearly continuously producing a vertical jet that has been previously documented (18–20), but not fully described and thus the ecological implications of this flow have not been addressed.

There is normally a downward flux of nutrients in sheltered coastal environments (21). therefore, an upward pump such as the one created by *Cassiopea* sp. may serve to increase nutrient levels in the water column by preventing settling of detritus (5) as well as by directly moving interstitial water into the water column (20), potentially altering local productivity.

In this study, we quantify the large scale flow features of

Significance Statement

Coastal mangrove habitats are vital nurseries for many commercial and ecologically important species. these habitats are sheltered from winds and tides, resulting in very little water mixing. The upside-down jellyfish, *Cassiopea* sp., occurs in mangrove habitats around the world at densities of up to 100 animals m^{-2}. Each jellyfish rests on the bottom pulsing nearly continuously and produces a vertical current that vertically transports hundreds of liters per hour of seawater. This results in turnover of the entire water column every 15 minutes in an average population. In addition, *Cassiopea* sp. can move water through nutrient-rich sediments and transport these nutrients into the water column. This study demonstrates that the upside-down jellyfish represents an previously unrecognized ecosystem engineer that may affect primary production and alter new habitats as their range is expanding.

[1]Authors contributed equally to this work.

[2]To whom correspondence should be addressed. E-mail: davidduriieux@mail.usf.edu

DRAFT

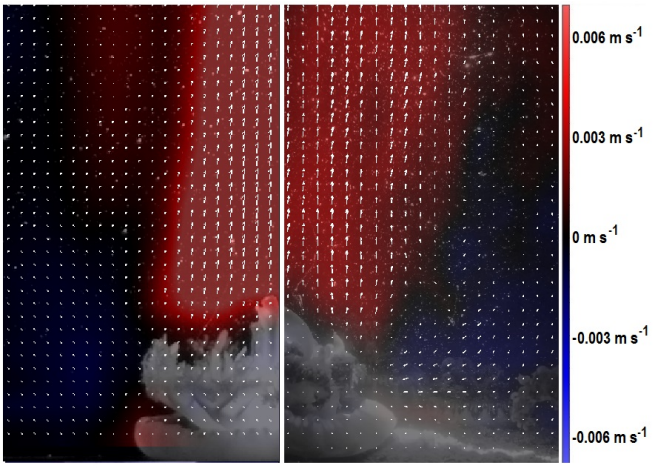

Fig. 1. Laboratory (left) and in-situ (right) Particle Image Velocimetry (PIV) of a representative *Cassiopea* sp. jet. White vector arrows show the direction of flow, with regions of upward (red) and downward (blue) flow. Features of this flow, including velocity and jet shape are similar between in-vitro and in-situ images.

individual *Cassiopea* sp. and small groups both in the lab and in the field. We examine the flows created by *Cassiopea* sp. in the context of the local environment and also quantify the ability of *Cassiopea* sp. to move water through the sediments, and discuss the release of nutrient rich interstitial pore water from sediments into the water column.

Results

Field Population. At our study site in the Florida Keys, USA, the density of the studied population of *Cassiopea* sp. ranged from 3 to 97 animals m^{-2}, with a median density of 29 animals m^{-2} (fig. 2). The sizes of these animals followed a Poisson distribution (fig. S1, Chi-Squared Test for Independence, $p < .001$) with a mean of 11.3 cm oral arm diameter (OAD). Since there is a linear relationship between OAD and resting bell diameter (RBD) (fig. S2, eq. 1 , $n = 50$, $R^2 = 0.9$), the mean RBD, weighted by frequency, can be estimated as 8.6 cm. The largest animal observed was 30 cm OAD (20.7 cm RBD). Based on morphological measurements of collected animals, animals with the observed average RBD of 8.6 cm can be assumed to have a wet weight of 56.5 g (fig. S2, eq. 2, $n = 50$, $R^2 = 0.99$) and a dry weight of 3.2 g (fig. S2, eq. 3, $n = 31$, $R^2 = 0.98$). These measurements will be considered to be an average animal.

Quantitative Description of the Vertical Jet. Particle Image Velocimetry (PIV) was performed on 9 *Cassiopea* sp. ranging in size from 4.8 cm – 14.5 cm RBD. Analysis of the shape of the jet produced by these animals showed that the jet diameter (D_j), relative to resting bell diameter (RBD), spreads linearly as height (Z) increases, (fig. S2, eq. 4, $R^2 = 0.64$). Maximum velocity showed the expected inverse relationship with height (fig. S2, eq. 5, $R^2 = 0.33$). Velocity at a height of 0 was roughly 20 mm s^{-1} regardless of bell diameter, but the rate of slowing decreased for larger animals. We can extrapolate upwards and find that, for the average animal (RBD = 8.6 cm) in the absence of other effects, the jet would slow to 0.5 mm s^{-1} at a height of 6.4 meters. Most animals in this site are found between 0.5 and 2 m deep, so their jets likely reach the surface in this habitat. In-situ PIV confirmed the experimental velocity, with the wild animal producing a flow of 12.4 mm s^{-1}.

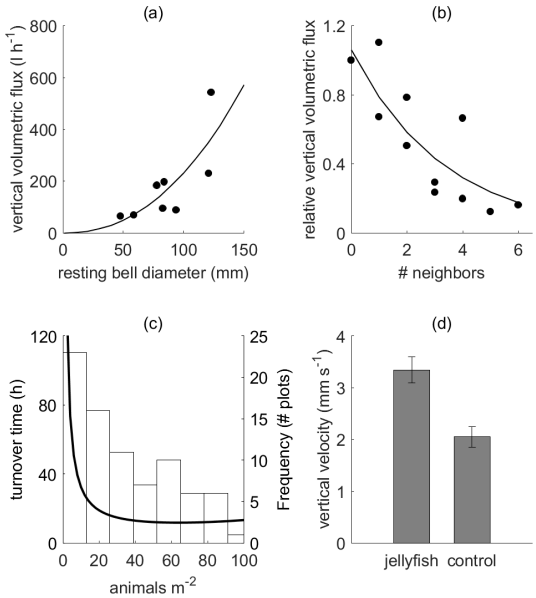

Fig. 2. (a) Vertical flux of water follows a power law relationship with animal size ($R^2 = 0.732$, n = 9). **(b)** The relative vertical flux, such that a value of one is equal to the amount an individual pumps in the absence of neighbors, decreases as the number of neighbors increases ($R^2 = 0.74$, n = 12).**(c)** Predicted time to turn over the column of water above a square-meter patch of *Cassiopea* sp. assuming a water depth of 1 meter, which was typical in our field site, relative to the population density in that patch. Frequency of different population densities observed is shown as a histogram of 1 m square plots. **(d)** Vertical flow component in the presence and absence of *Cassiopea* sp. at Lido Key, Florida. The presence of *Cassiopea* sp. increased vertical flow (Unpaired t-test, $p \leq 0.001$)

Flux and Turnover Time. At a distance of two bell diameters above the animals, vertical velocity was found to be independent of bell diameter, as was expected from the observation of jet shape. Because jet diameter was found to correlate directly with bell diameter, and velocity was independent of bell diameter, vertical flux of water (Q) was found to follow a power law function relative to resting bell diameter, with a power of 2.23 (fig. 2a; fig. S2, eq.6, $n = 9$, $R^2 = 0.74$). The relationship can also be expressed as weight-specific flux (F) in terms of dry weight (fig. S2, eq. 7). The average *Cassiopea* sp. moves 212 l h^{-1} of seawater, a mass-specific volumetric flow rate of 62.9 l h^{-1} g^{-1} dry weight (DW), with the smallest animals producing 200 to 600 l h^{-1} g^{-1} DW, indicating an allometric scaling process.

Since *Cassiopea* sp. form aggregations a correction factor was needed to account for interactions between individuals. The jet of an individual *Cassiopea* sp.was examined under conditions with different numbers of neighbors, and the flux was found to decrease with the addition of each neighbor (fig. 2b; fig. S2, eq. 8). Based on to photographic transects of the

DRAFT

Table 1. Estimated filtration rate per individual, as well as wet weight and dry-weight specific filtration rates for *Cassiopea* sp. (assuming a density of 29 animals m^{-2}), *C. virginica*, and *M. edulis*. Rates for *Cassiopea* sp. are consistently an order of magnitude larger than those of bivalves. Citations refer to sources of filtration rates and size conversion factors used to calculate these values.

	Filtration Rate (l h^{-1})	WW-Specific Filtration Rate (l h^{-1} g^{-1})	DW-Specific Filtration Rate (l h^{-1} g^{-1})
Cassiopea sp. (Current Study)	137	2.43	42.89
Crassostrea virginica	2.61 (22, 23)	0.71 (23, 24)	6.41 (23)
Mytilus edulis	11.9 (9)	0.80 (9, 25, 26)	5.94 (9, 26)
Ciona intestinalis	0.1 to 1 (27)	1.16 to 1.57 (27, 28)	24 (28)

field population in the Florida Keys, at the median density of 29 animals m^{-2}, each animal will have an average of 1.23 neighbors (fig. S2, eq. 9). Assuming a water depth of 1 meter, which was fairly typical at the field site, the turnover time for the water column can be calculated for varying population densities by dividing the water volume by the sum of the fluxes of the animals on the bottom under that volume. A single animal would turn over this water column in 4.7 hours. At the observed median population of 29 animals m^{-2} the resulting flux is 3980 l h^{-1}, and the calculated turnover time is reduced to 15 minutes. Turnover time decreases as population density increases to a minimum of 11.8 minutes at a density of 64 animals m^{-2} (Fig. 2c)

In Situ Flow Measurement. In the Lido Key site, measurements of flow in habitat occupied by *Cassiopea* sp. using an Nortek Vector Acoustic Doppler Velocimeter demonstrated that *Cassiopea* sp. increase vertical transport of water in these habitats. Mean vertical velocity increased from 2.1 mm s^{-1} in the absence of jellyfish to 3.3 mm s^{-1} directly over patches of jellyfish (Fig. 2d).

Interstitial Water Release. Fluorescein concentrations increased visibly in the trials that included a jellyfish but not in controls. The average flow attributed to a single jellyfish, normalized to an RBD of 8.6 cm, amounted to 2.64 ml h^{-1} of interstitial water released into the water column (Fig. 3), while trials without jellyfish had no fluorescein release. The flow rate in the presence of jellyfish was found to vary significantly from zero (1-Sample t-test, $p = 0.0055$). Interstitial water release rate increased linearly with bell diameter. (Fig. 3, $n = 9$, $R^2 = 0.3622$)

Discussion

In most coastal ecosystems, wind and tidal flow are the primary mixing forces (10). However, the systems inhabited by *Cassiopea* sp. are sheltered by dense stands of *Rhizophora* mangrove trees, reducing wind-water interaction in these lagoons and estuaries. In addition, *Cassiopea* sp. dwell outside of the tidal streams, where most tidal flushing in these habitats occurs (4), residing rather on the adjacent flats. Together, these two habitat features result in a system with

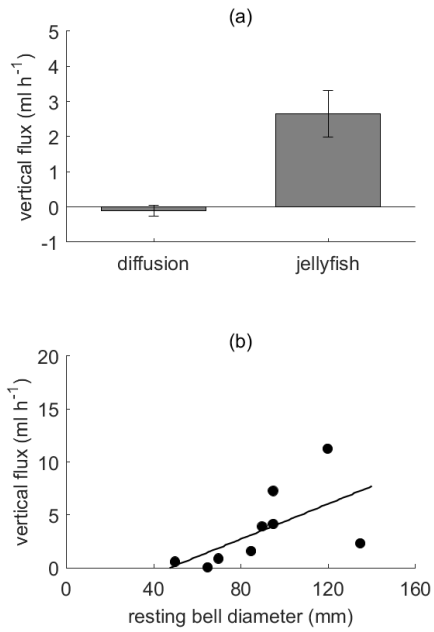

Fig. 3. (a) Vertical flux of interstitial water out of the sediment attributed to a single *Cassiopea* sp., normalized to a resting bell diameter of 8.6 cm (the average observed in the field), compared to the rate due to diffusion in the experimental container. Interstitial water release due to diffusion was negligible, while the average *Cassiopea* sp. released 2.6 ml h^{-1}. **(b)** Vertical flux of interstitial water relative to bell diameter. As animal size increased, the interstitial flow increased as well ($n = 9$, $R^2 = 0.3622$).

comparatively little physical mixing. This low energy habitat is further evidenced by the presence of a fine-grain benthic substrate in the areas where *Cassiopea* sp. are abundant (29). Our results from field measurements near *Cassiopea* sp. habitats found turbulent kinetic energy (TKE) values at 20-30 cm above the bottom to be 5x10^{-5} m^{2}s^{-2} (fig. 2d) which was nearly an order of magnitude lower than previously reported measures of 4x10^{-4} m^{2}s^{-2} (30). This confirmed that environmental flow conditions in *Cassiopea* sp. habitat were both low, with little mixing. As such, the cumulative effect of a population of *Cassiopea* sp. has the potential to provide a large contribution to mixing, relative to non-biogenic factors, which may have important ecological implications.

Our estimates show that given the observed slowing rate (fig. S2, eq. 5), the average animal could produce a jet on the order of several meters tall, which will affect the entire depth of the water column (0.5 m to 2 m) in the shallow system where *Cassiopea* sp. occur. This mixing contribution is higher than is observed in other species (Table 1). Our results indicate that an individual average-sized animal can move 212 l h^{-1} of seawater upward in its vertical jet (Fig. 2a). After factoring in the effect of neighboring animals, our model predicts that the median population density observed in our field site (29 animals m^{-2}) can turn over a 1 m deep column every 15 minutes (fig. 2c). By comparison, the mussel *M. edulis* has been observed to move 6.4 - 11.9 l h^{-1} (9), which is far below the rates measured in *Cassiopea* sp.

To account for differences in body mass, weight-specific

DRAFT

filtration rates can also be compared (table 1). The eastern oyster *Crassostrea virginica* moves 6.4 l h^{-1} g^{-1} dry weight (23). *Cassiopea* sp. in this study exhibited volumetric flow rates over 10 times those of *C. virginica* by dry weight. Therefore, per square meter of benthos, *Cassiopea* sp. act as much more effective water pumps than do bivalves. Weight-specific filtration rates have also been calculated for the tunicate *Ciona intestinalis*, at 24 l h^{-1} g^{-1} dry weight (28). This puts the pumping rate of tunicates at a level closer to that of *Cassiopea* sp., likely due to the fact that it, like *Cassiopea* sp., has a high water content, its dry weight being 15-20 times less than its wet weight. However, due to the much smaller size of *C. intestinalis*, they move a lower magnitude of water than *Cassiopea* sp. overall.

Since pumping rate is known to scale allometrically with size, more meaningful comparisons may be drawn from the shape of the scaling equation that relates volumetric flow rate to body mass. The exponent of this function is roughly $\frac{2}{3}$ for *Cassiopea* sp. (fig. S2, eq. 7), as for most species, indicating that pumping rate scales with surface area, rather than volume or length (31, 32), but differences can be seen between *Cassiopea* sp. and other pumping species in terms of the coefficient of the scaling equation. This study found a coefficient of 96.89 in *Cassiopea* sp. (fig. S2, eq. 7), compared to 6.79 in *Crassostrea virginica* and 7.45 in *Mytilus edulis* (31). Since the exponents are comparable, we can conclude that a *Cassiopea* sp. of a given dry weight will move roughly 10 to 20 times as much water as an equivalently sized bivalve. Added to the fact that *Cassiopea* sp. can grow much larger than bivalves (up to 30 g DW) we can show that *Cassiopea* sp. are stronger 'pumps' than the more well-studied bivalves.

Of course, animals such as oysters and mussels can occur at much higher densities than *Cassiopea* sp. do, but their relatively small individual flow is not fully compensated for in terms of numbers. High densities of over 700 animals m^{-2} have been reported for *Mytilus edulis* (33) and *Crassostrea virginica* (22). Assuming adult, 50 mm (or 0.3g dry weight (22)) oysters and additive contributions, which is almost certainly an overestimate, this would produce approximately 1176 l h^{-1} m^{-2} flow. Using 1.5 g dry weight for an adult mussel (26) and the same assumptions, we calculate a flow of 3443 l h^{-1} m^{-2}. Our median population of *Cassiopea* sp. (29 animals m^{-2}) moved 3980 l h^{-1} m^{-2}, while the maximum density observed in this study moved 4569 l h^{-1} m^{-2}. Thus, *Cassiopea* sp. populations, despite their lower population densities, are responsible for much greater amounts of water transport than are bivalve reefs.

The tunicate *Ciona intestinalis*, which has a relatively high weight-specific filtration rate, was found to pump water at rates of 0.1 to 1 l h^{-1}(27). This species, which has been recorded at densities of over 1000 individuals m^{-2}(34), could therefore have a population filtration rate on the order of 1000 l h^{-1} m^{-2}, comparable to oysters, but still much lower than *Cassiopea* sp.İn addition, *Cassiopea* sp., unlike other biological pumps that are smaller, are capable of producing jets which reach the surface of the water(fig. S2, eq. 5).

There are also other ways that *Cassiopea* sp. populations may alter their environments. An increase in mixing, especially the upward vertical transport produced by a vertical jet, should lead to a decrease in sedimentation in low-energy habitats. Particulates in mangrove habitat flocculate, increasing particle size, but the low density of these flocs reduces sedimentation rate (35). *Cassiopea* sp. themselves may contribute to flocculation by the production of mucus (13), which traps suspended particles (35). These particles may be further prevented from settling by addition of mixing energy by *Cassiopea* sp. increasing turbidity.

Increasing mixing from the bottom up can also impact water column production. For example, a mesocosm study where mixing was initiated close to the bottom, as is the case with *Cassiopea* sp., found that faster turnover resulted in longer-lasting algae blooms and higher chlorophyll concentrations than at lower mixing rates (36), likely because of the increased availability of nutrients to phytoplankton cells.

It has been previously demonstrated that *Cassiopea* sp. can transport interstitial pore water in sediments from several cm deep in the benthos to the water column (20) but volume fluxes were not measured. In Gulf of Mexico sediments, increasing the advective benthic flow produced an increase in denitrification rates (37) so it is possible that *Cassiopea* sp. can also contribute to increased denitrification. Our results show that an average-sized animal (8.6 cm) would release approximately 2.6 ml h^{-1} of porewater (fig. 3, and the median population of 29 animals m^{-2} would therefore release 1809.6 ml day^{-1}. Given that these animals tend to move slowly over the bottom, thereby encountering new sediments regularly, and the reported phosphate and nitrogen concentrations in the sediment (38) at Long Key, Florida, this could release roughly 0.34 mg day^{-1} m^{-2} of NO_3, 2.35 mg day^{-1} m^{-2} of NH_4, and 1.03 mg day^{-1} m^{-2} of PO_4. Since these released nutrients will be mixed into the water column upon becoming entrained in the vertical jets and assuming a 1 m water depth, this represents an increase of 29% in water column NH_4, a 6% increase in PO_4, and a 0.5% increase in NO_3 relative to reported water column nutrient concentrations from these habitats (38). The addition of the mixing contribution produced by *Cassiopea* sp. into a habitat with low environmental water mixing, as well as a substantial release of interstitial water leading to an additional source of nutrients in this ecosystem, make it likely that *Cassiopea* sp. are previously unrecognized ecosystem engineers within mangrove habitats.

Materials and Methods

Field Population. The field study site on Long Key, Florida, USA (24.527 N,-80.814 W) was sheltered by red mangroves (*Rhizophora mangle*) and held a population of *Cassiopea* sp. at depths ranging from 0.5 to 2 m deep. The benthic habitat where *Cassiopea* sp. were most abundant consisted of very fine sediment, surrounded by seagrass (*Thalassia* and *Syringopodium*).

The population structure of a natural *Cassiopea* sp. population was quantified during December 2016, by setting two transects through the patch, 10 meters apart, parallel to one another in a roughly east-west orientation. Quadrats of 1 m^2 were sampled every 1.5 m on each transect to reduce investigator bias in selecting animals for measurement. Each quadrat was photographed from above, and the oral arm diameter (OAD) of each animal was

DRAFT

measured from these images by measuring the longest observable distance from one oral arm tip to another oral arm tip. During the summer of 2017, fifty animals were collected and imaged from above and from the side. The resting bell diameter (RBD, used for lateral imaging) was measured during the resting phase between bell contractions, and was correlated to the OAD, wet weight (WW), and dry weight (DW) by linear regression to allow conversion between measurements. Based on these parameters, populations of *Cassiopea* sp. at different densities were calculated.

Vertical Jet Imaging. To determine the volumetric flow rate of vertical water movement, the vertical jet must first be described quantitatively. *Cassiopea* sp. of various sizes were collected from the Keys Marine Laboratory on Long Key, Florida, USA during the month of December, 2016 and August, 2017, and transported in collected seawater back to the University of South Florida, in Tampa, Florida, where they were housed in a 300 liter closed loop aquarium system. The animals were kept in artificial seawater mixed to a salinity of 35‰ with Instant Ocean aquarium salt, over a substrate of aragonite sand and high intensity metal halide lighting on a 12:12 light cycle.

The imaging setup consisted of a 45 x 45 x 45 cm aquarium, filled with artificial seawater at 35‰ salinity. The water was seeded using 10 μm reflective hollow glass spheres for particle image velocimetry (PIV). An Edgertronic high-speed camera filming at 50 frames per second provided a field of view ca. 30 cm x 30 cm. Two 2-watt continuous wave DPSS lasers (wavelength = 520 nm), spread through cylindrical lenses to produce narrow light sheets, were staggered one above the other to illuminate a single coronal plane across the entire field of view. One jellyfish at a time (n = 9) was placed on the bottom in the center of the aquarium, such that the laser sheet crossed the center of the animal. After allowing it to settle for about 10 minutes, 30 seconds of video were recorded at 50 frames per second. At least five such image sequences were made, and the three with the most similar pulse rates were retained for analysis using the LaVision software package, producing a PIV time-average over the 30 seconds. PIV was processed with interrogation windows between 48 and 64 pixels, at 50% overlap.

A custom MATLAB script was used to identify and measure the vertical jet from this time average. The location of the jet was defined as the region where the vertical velocity was greater than 0.5 mm s^{-1}. This region was used to calculate the jet diameter. Due to the asymmetric meandering of the jet, volumetric flux was calculated by using a variant of the washer method. We integrate vertical velocity between the edges of the jet, using half-washers on each side of the position of maximum upward velocity (fig. 1). Because of the high degree of irregularity in *Cassiopea* sp. jets, the three image sequences of each animal were combined to create a single representative jet by taking the median values for jet diameter, jet area, maximum and average Vz, and vertical volumetric flux (Q) at each height for use in further analysis.

This method produces an artificial tapering of the jet shape towards its highest end due to the fixed velocity threshold, since the maximum velocity of the jet approaches the minimum threshold as it slows with increasing height. To account for this, data above the height of the maximum measured jet diameter were excluded. In addition, the development region of a turbulent jet does not follow the same patterns as the fully developed region (39). To take this into account, the lowest data points were excluded so that the data series always began at a local maximum in Vz.

For confirmation of the laboratory results, in-situ PIV was performed at the field site. A Nikon D750 DSLR at 50 frames per second camera in an underwater housing was lined up the bottom near an individual *Cassiopea* sp. with a green laser, spread through a cylindrical lens, also housed in a water-tight case. PIV analysis using the naturally-occurring particles was performed using DaVis, and the time-averaged velocities compared to those measured in the laboratory.

Quantitative Description of the Vertical Jet. Upward velocity (Vz) was expected to show an inverse relationship (39) with height (Z) relative to resting bell diameter (RBD) (fig. S2, eq. 10). In addition, the jet diameter (D_j) relative to RBD was hypothesized to increase linearly over this region (39) (fig. S2, eg. 11). Vertical volumetric flux (Q) was expected to increase linearly with height, due to entrainment of water into the turbulent jet, and increase linearly with animal size (39). The resulting equation is a function of average velocity and jet diameter(fig. S2, eq. 12). These relationship were tested using the Nonlinear Regression tool in SPSS statistical software version 23.

To confirm that *Cassiopea* sp. in the field produce the same vertical jet as animals in a captive setting, in-situ PIV was performed on an animal at the Keys Marine lab, and the parameters of this jet were compared to those captured in the laboratory.

Weight-specific volumetric flow rates were calculated by calculating the expected flux of the animals used for morphological measurements, and then expressing this flux in terms of the wet and dry weights of those animals.

Interactions Between Multiple Animals. Because *Cassiopea* sp. are often found in dense aggregations, we determined the degree of interference between adjacent animals using the same PIV design. A single animal was placed in the filming vessel, and then surrounded by an increasing number of neighbors. The vertical velocity and diameter of the original animal's jet were calculated as before, allowing us to determine the degree of inhibition caused by the addition of neighbors. This was compared to the number of neighbors expected in wild populations, determined from the same transect photos used to determine average animal size and population density.

Turnover Time. The time needed for a *Cassiopea* sp. population to turn over the water column above it, where the jet reached the surface, was calculated by taking the volume of water above a 1 m^2 patch of a hypothetical *Cassiopea* sp. population and calculating the vertical volumetric flux for each animal in that population. The sum of the vertical flux rates (Q) of the animals in this hypothetical patch is divided by the volume of water, giving the turnover rate (fig. S2, eq. 13).

In Situ Flow Measurement. Flow velocities were measured around a population of *Cassiopea* sp. at Lido Key, Florida, (27.303 N, -82.566 W) using an Nortek Vector Acoustic Doppler Velocimeter (ADV), facing downward, suspended over the benthos with a focal region 20-30 cm above the bottom, sampling at a rate of 8 Hz. We deployed the ADV over areas with high *Cassiopea* sp. density, as well as in similar adjacent regions without *Cassiopea* sp.. The resulting velocity vectors were filtered to remove any vectors with velocity of over 10 cm/s, which was determined to be above the range produced by both ambient flow and *Cassiopea* sp., according to our PIV data. This was done to remove signals from small fish that used the ADV mount as structure.

Interstitial Water Release Rates. We labeled play sand by mixing it with a solution of fluorescein in artificial seawater until the sand was uniformly damp. A layer of labeled sand 2.5-3 cm deep was added to the bottom of an 8 l plastic bucket in a larger water bath, and gently pressed down to smooth. Over this layer we added a layer of clean play sand mixed with seawater at a rate of 500 ml seawater to 2 l of dry sand. This unlabeled layer was ca. 1 cm thick, which delayed leaching of fluorescein into the water column by about 30 minutes. The bucket was then gently filled by pumping 4 liters of artificial seawater slowly over a petri dish to prevent disturbance of the sand layers. Immediately after filling we took samples of interstitial and column water. A *Cassiopea* sp. specimen

DRAFT

was then placed on the sand in the center of the bucket. For each experimental day, one trial was performed without a jellyfish to measure diffusion rates in the absence of animals. At two and three hours, additional water samples were taken and the absorbance at 494 nm compared to a dilution curve of the interstitial water sample taken at the start of each experiment. The fluorescein concentrations at each time were corrected by subtracting the measured concentrations of the starting water sample for the same trial, and the concentration of the control experiment at the same time point. These corrected values were then used to calculate the rate of interstitial water release into the water column.

ACKNOWLEDGMENTS. The authors would like to acknowledge the following people who assisted with specimen collection and experimentation (in alphabetical order): Olivia Blondheim, Alicia Durieux, Christian Fender, Olivia Hawkins, Kathrene Lo, Gabrielle Scrogham, Nils Tack. Additionally, we would like to thank the Keys Marine Laboratory for use of their facilities. Funding for this project was provided by the National Science Foundation (Grant XXX).

1. Gilbert AJ, Janssen R (1998) Use of environmental funtions to communicate the values of a mangrove ecosystem under different management regimes. *Ecological Economics* 25:323–346.
2. Das S (2017) Ecological Restoration and Livelihood: Contribution of Planted Mangroves as Nursery and Habitat for Artisanal and Commercial Fishery. *World Development* 94:492–502.
3. Robertson AI, Duke NC (1987) Mangroves as nursery sites: comparisons of the abundance and species composition of fish and crustaceans in mangroves and other nearshore habitats in tropical Australia. *Marine Biology* 96:193–205.
4. Wolanski E, Mazda Y, Ridd P (2013) Mangrove Hydrodynamics in *Tropical Mangrove Ecosystems*, eds. Alongi AR, D.M. (American Geophysical Union) Vol. 41, pp. 43–62.
5. Lawrence D, et al. (2004) Wind events and benthic – pelagic coupling in a shallow subtropical bay in Florida. *Marine Ecology Progress Series* 266:1–13.
6. Ackerman JD, Loewen MR, Hamblin PF (2001) Benthic pelagic coupling over a zebra mussel reef in western Lake Erie. *Limnology and Oceanography* 46(4):892–904.
7. Katija K, Dabiri JO (2009) A viscosity-enhanced mechanism for biogenic ocean mixing. *Nature* 460(7255):624–626.
8. Huntley ME, Zhou M (2004) Influence of animal on turbulence in the sea. *Marine Ecology Progress Series* 273:65–79.
9. Riisgård HU, et al. (2011) The exhalant jet of mussels *Mytilus edulis*. *Marine Ecology Progress Series* 437(September):147–164.
10. Jones NL, Monismith SG (2008) Modeling the influence of wave-enhanced turbulence in a shallow tide- and wind-driven water column. *Journal of Geophysical Research: Oceans* 113(3):1–13.
11. Holland BS, Dawson MN, Crow GL, Hofmann DK (2004) Global phylogeography of *Cassiopea* (Scyphozoa: Rhizostomeae): Molecular evidence for cryptic species and multiple invasions of the Hawaiian Islands. *Marine Biology* 145(6):1119–1128.
12. Fleck J, Fitt WK (1999) Degrading mangrove leaves of *Rhizophora mangle* (Linne) provide a natural cue for settlement and metamorphosis of the upside down jellyfish *Cassiopea xamachana* (Bigelow). *Journal of Experimental Marine Biology and Ecology* 234(1):83–94.
13. Niggl W, Wild C (2010) Spatial distribution of the upside-down jellyfish *Cassiopea sp.* within fringing coral reef environments of the Northern Red Sea: Implications for its life cycle. *Helgoland Marine Research* 64(4):281–287.
14. Morandini AC, Stampar SN, Maronna MM, Da Silveira FL (2016) All non-indigenous species were introduced recently? The case study of Cassiopea (Cnidaria: Scyphozoa) in Brazilian waters. *Journal of the Marine Biological Association of the United Kingdom* 97(2):1–8.
15. Keable SJ, Ahyong ST (2016) First Records of the Invasive "Upside-down Jellyfish", *Cassiopea* (Cnidaria : Scyphozoa : Rhizostomeae : Cassiopeidae), from Coastal Lakes of New South Wales, Australia. *Records of the Australian Museum* 68:23–30.
16. Özgür E, Öztürk B (2008) A population of the alien jellyfish, *Cassiopea andromeda* (Forsskål, 1775) (Cnidaria: Scyphozoa: Rhizostomea) in the Ölüdeniz Lagoon, Turkey. *Aquatic Invasions* 3(4):423–428.
17. Stoner EW, Layman CA, Yeager LA, Hassett HM (2011) Effects of anthropogenic disturbance on the abundance and size of epibenthic jellyfish *Cassiopea spp.* *Marine Pollution Bulletin* 62(5):1109–1114.
18. Hamlet CL, Miller LA, Rodriguez T, Santhanakrishnan A (2012) The fluid dynamics of feeding in the upside-down jellyfish. *Natural locomotion in fluids and on surfaces; swimming, flying and sliding (IMA)* 155:35–51.
19. Santhanakrishnan A, Dollinger M, Hamlet CL, Colin SP, Miller LA (2012) Flow structure and transport characteristics of feeding and exchange currents generated by upside-down *Cassiopea* jellyfish. *Journal of Experimental Biology* 215:2369–2381.
20. Jantzen C, Wild C, Rasheed M, El-Zibdah M, Richter C (2010) Enhanced pore-water nutrient fluxes by the upside-down jellyfish *Cassiopea sp.* in a Red Sea coral reef. *Marine Ecology Progress Series* 411:117–125.
21. Morell JM, Corredor JE (1993) Sediment Nitrogen trapping in a mangrove lagoon. *Estuarine, Coastal and Shelf Science* 37(2):203–212.
22. Mann R, Southworth M, Harding JM, Wesson JA (2009) Population Studies of the Native Eastern Oyster, *Crassostrea virginica* , (Gmelin, 1791) in the James River, Virginia, USA. *Journal of Shellfish Research* 28(2):193–220.
23. Newell RIE, Koch EW (2004) Modeling seagrass density and distribution in response to changes in turbidity stemming from bivalve filtration and seagrass sediment stabilization. *Estuaries* 27(5):793–806.
24. Mo C, Neilson B (1994) Standardization of oyster soft tissue dry weight measurements. *Water Research* 28(1):243–246.
25. Phillips DJH (1976) The common mussel *Mytilus edulis* as an indicator of pollution by zinc, cadmium, lead and copper. I. Effects of environmental variables on uptake of metals. *Marine Biology* 38(1):59–69.
26. Dare PJ, Edwards DB (1975) Seasonal changes in flesh weight and biochemical composition of mussels (*Mytilus edulis* L.) in the Conwy Estuary, North Wales. *Journal of Experimental Marine Biology and Ecology* 18(2):89–97.
27. Du Clos KT, Jones IT, Carrier TJ, Brady DC, Jumars PA (2017) Model-assisted measurements of suspension-feeding flow velocities. *The Journal of Experimental Biology* 220(11):2096–2107.
28. Petersen JK, Svane I (2002) Filtration rate in seven Scandinavian ascidians: Implications of the morphology of the gill sac. *Marine Biology* 140(2):397–402.
29. Leonard LA, Luther ME (1995) Flow hydrodynamics in tidal marsh canopies. *Limnology and Oceanography* 40(8):1474–1484.
30. Zhang X, Chua VP, Cheong HF (2015) Hydrodynamics in mangrove prop roots and their physical properties. *Journal of Hydro-Environment Research* 9(2):281–294.
31. Riisgård HU (2001) On measurement of filtration rate in bivalves-the stony road to reliable data: review and interpretation. *Marine Ecology Progress Series* 211:275–291.
32. Officer CB, Smayda TJ, Mann R (1982) Benthic filter feeding: A natural eutrophication control. *Marine Ecology Progress Series* 9:203–210.
33. McGrorty S, Clarke RT, Reading CJ, Goss-Custard JD (1990) Population dynamics of the mussel *Mytilus edulis*: density changes and regulation of the population in the Exe estuary, Devon. *Marine Ecology Progress Series* 67(Holm):157–169.
34. Svane I (1983) Ascidian reproductive patterns related to long-term population dynamics. *Sarsia* 68(4):249–255.
35. Wolanski E (1995) Sediment transport in mangrove swamps. *Hydrobiologia* 295:31–42.
36. Petersen JE, Sanford LP, Kemp WM (1998) Coastal plankton responses to turbulent mixing in experimental ecosystems. *Marine Ecology Progress Series* 171:23–41.
37. Gihring TM, Canion A, Riggs A, Huettel M, Kostka JE (2010) Denitrification in shallow, sublittoral Gulf of Mexico permeable sediments. *Limnology and Oceanography* 55(1):43–54.
38. Szmant AM, Forrester A (1996) Water column and sediment nitrogen and phosphorus distribution patterns in the Florida Keys, USA. *Coral Reefs* 15(1):21–41.
39. Pope SB (2000) Free Shear Flows in *Turbulent Flows*. (Cambridge University Press), pp. 96–134.

DRAFT